International Journal of Engineering &Technology, 13 (1) (2024) 76-86

International Journal of Engineering & Technology

Website: www.sciencepubco.com/index.php/IJET

Research paper

Mathematical modeling transfers during convective drying of papaya (carica papaya l.) considering the boundary conditions at the leading and trailing edges

Fouakeu-nanfack Gildas Armel [1] *, Tetang Fokone Abraham [1], Ekani Roger Yannick [1, 2, 3], Tientcheu Nsiewe Maxwell [1], Edoun Marcel [1], Kuitche Alexis [1], Ze-ghmati Belkacem [4]

[1] *Laboratory of Energetics and Applied Thermal, ENSAI-University of Ngaoundere, Cameroon.*
[2] *National Advanced school of Maritime and Ocean Science and Technology (NASMOST) of the University of Ebolowa, Cameroon*
[3] *Laboratory E3M, National Higher Polytechnic School of Douala, University of Douala, Cameroon*
[4] *Laboratory of Mathematics and Physics (LA.M.P.S), University of Perpignan via Domitia, France*
**Corresponding author E-mail: fouakeunanfack@gmail.com*

Abstract

In this study, convective heat and mass transfer during papaya drying in a parallel airflow were simulated. The aim of this work was to con-sider the boundary conditions at the leading and trailing edges in the coupled and simultaneous resolution of the heat and mass transfer equations to better predict papaya drying kinetics. The Luikov equations established for this transfer model were discretized by the implicit finite-difference method and then solved simultaneously using the MATLAB 2014 tool. The drying process was simulated under the influence of drying air conditions and product thickness. The results showed that for the moisture ratio, the mean relative errors were 5.21% and 3.89% for the model without and with boundary conditions set at the leading and trailing edges, respectively. Similarly, the results showed that for product temperature, the mean relative errors were 4.35% and 3.61% for the model without and with boundary conditions set at the leading and trailing edges, respectively. Comparison of the predicted models with the experimental data satisfactorily demonstrated that in-corporating the leading and trailing edge boundary conditions in a transfer model enabled better prediction of drying kinetics than the model without the leading and trailing edge boundary conditions.

Keywords: *Boundary Conditions; Convective Drying; Leading and Trailing Edge; Mathematical Modeling; Transfers.*

1. Introduction

Many agricultural products are not always in season, including the vast majority of fruits and vegetables that we consume. These produce items' high vitamin and mineral contents make them a significant source of vitamins and minerals for human nutrition [1]. Most of these products are gathered when the relative humidity is very high. Due to the perishable nature of the product and its susceptibility to various contaminations (molds, germs, etc.), it must be sold or consumed fresh within a very short amount of time [2]. If not, it deteriorates and ceases to be fit for eating. Small-scale farmers who rely on their meager plots of land for their livelihood are also susceptible to market fluctuations, especially during the growth seasons when prices decline to the point where production is in deficit. Many approaches have been proposed to overcome this difficulty, including greenhouse cultivation, freezing, and drying [3]. Drying is a rapid, safe, and efficient technique for reducing postharvest loss. According to [4], drying is a process used to partially or completely evaporate the water from a moist body. This technique can increase the shelf life of most food crops in Sub-Saharan African nations, especially those with high moisture contents (moisture content between 60 and 90%), which are particularly perishable items [5]. Convective drying, which removes moisture from a product by blowing hot air over it using static dryers powered by electricity or solar energy [6], is one of the most commonly utilized techniques [7]. Despite numerous optimization efforts, this drying mode, which causes heat and mass transfer, still consumes a significant amount of energy. If this drying mode is to be improved, it is essential to accurately predict the transfer phenomena as well as the quality of the products. In order to predict the drying kinetics, Stegou-Sagia and Fragkou [8], Fernando and Amarasinghe [9], Stegou–Sagia and Fragkou [10], Badaoui et al. [11], Tetang et al. [12], Tom et al. [13], Keskes et al. [14], Kushwah et al. [15], Fouakeu-nanfack et al. [16], Wang et al. [17] and Oladejo et al. [18] have performed empirical and semi-empirical modeling of the drying of agri-foodstuffs in thin films. However, the application of these models is constrained because each of them is unique to the type of product and the drying experiment conditions. Therefore, these models cannot be extrapolated from experimental parameters. A different strategy is theoretical modeling, which entails understanding the multiple intricate mechanisms of heat and mass exchanges that take place within the product [2]. The complexity of the systems under study frequently causes oversimplification of some assumptions. The reduction of convective drying equations in one dimension (1D) [5], [19]–[22] and in two dimensions (2D) [23]–[26] has been widely explored to contribute to the improvement of transfer models. In the same concern to simplify these equations, Lagunez-Rivera et al. [27], Mocelin et al. [28], Torki-

Copyright © Fouakeu-nanfack Gildas Armel et al. This is an open access article distributed under the Creative Commons Attribution License, which permits unrestricted use, distribution, and reproduction in any medium, provided the original work is properly cited.

Harchegani et al. [29] and Dotto et al. [30] consider moisture transfer as the main phenomenon that occurs during the drying of food products, neglecting heat transfer. Although the individual transfer pattern is still used because of its simplicity for drying, it should be avoided because the effect of temperature is important for moisture transport. A simultaneous and coupled model taking into account mass and heat transport is more suitable for the convective drying of fruits. This approach has been widely used by Shahari et al. [25], Chasiotis et al. [21], Muhury et al. [31], Nasri and Belhamri [22], Chen et al. [32] and Souza et al. [33] over the past five years. An analysis of the various mean relative errors from the literature, in particular from prior work, has demonstrated that there is good agreement between experimental drying data and simulated data (mean relative errors ranging from 4 to 11%). It is necessary to enhance the heat and mass transfer prediction models for convective drying because this error should be less than or equal to 3%. An in-depth analysis of previous work Villa-Corrales et al. [34], Takamte et al. [35], Afolabi and Agarry [36], Shahari et al. [25], Erko et al. [19], Yu et al. [37], Chasiotis et al. [21], Muhury et al. [31], Nasri and Belhamri [22] and Fouakeu-nanfack et al. [38] shows that in many cases, boundary conditions are always set at the product surface and at the symmetrical center of the product, neglecting those that can be set at the leading and trailing edges of the product. This is one of the interests presented by our work, as very few works in the literature do not take into account the boundary conditions established at the leading and trailing edges when modeling coupled and simultaneous heat and mass transfers during the drying of food products.

2. Methods

2.1. Experimental device

The experiments were performed using a lab-scale convective drying air stream. Depending on the arrangement of this drying air stream, the products are exposed to a licking air flow. Air was blown into this dryer by an electric fan. The airflow velocity is regulated by a rheostat and measured using a hot-wire anemometer. The relative humidity was controlled via a data controller. The experiment included up to 8 hours of drying, and the weight of the samples was continuously recorded at predetermined intervals. The experimental tool that was used is described by Fouakeu-nanfack et al. [16].

2.2. Physical modeling of papaya drying

The system studied, illustrated on figure 1 below, is a wet product arranged on a support with the properties of papaya (Carica papaya L.), with a length of 30 cm and a thickness of 5 mm. The product's vertical sides are thought to be adiabatic and material-impermeable. The permeable interface, which is exposed to a hot air flow parallel to the product's free surface, is represented by the product's two upper and lower sides. At the product intake, it was assumed that the drying conditions of hot air (airflow velocity V_a, temperature of air T_a, and mass fraction C_{va}) were constant. The following figure shows the coordinate system used.

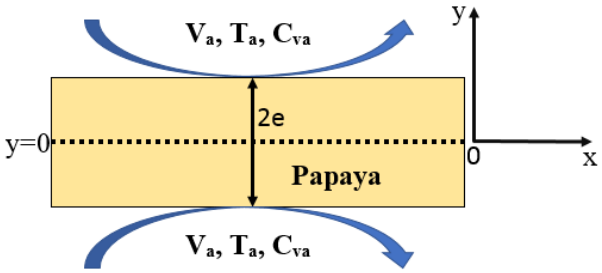


Fig. 1: Physical Modeling of Drying Papaya.

2.3. Hypotheses

We assume the following assumptions to streamline the formulation of the equations [26]:

- Problem is fully symmetrical about the median plane;
- Fluid is incompressible and Newtonian;
- Flow regime is turbulent and stationary;
- Deformation of the product during drying is neglected;
- Physical properties of the product and the air are variable;
- Radiative exchanges inside the chamber are neglected;
- Temperature and moisture content of the products were initially uniform.

2.4. Mathematical formulation of transfer equations

The heat and mass transfer equations used in the model are governed by the following two-dimensional partial differential equation (PDE) Kosheleva et al. [39], Matuam et al. [26] and Fouakeu-nanfack et al. [38]:

- Mass transfer equation

$$\frac{\partial X_p}{\partial t} = D_{eff}\left(\frac{\partial^2 X_p}{\partial x^2} + \frac{\partial^2 X_p}{\partial y^2}\right) \quad (1)$$

- Heat transfer equation

$$\rho_p C_{pp} \frac{\partial T_p}{\partial t} = \lambda_p\left(\frac{\partial^2 T_p}{\partial x^2} + \frac{\partial^2 T_p}{\partial y^2}\right) \quad (2)$$

Where C_{pp} is specific heat of the mass of product (kJ/kg °C); D_{eff} is effective diffusivity coefficient (m^2/s); T_p is temperature of product (°C); X_p is moisture content of the product ($kg/kg._{db}$); ρp is density of product (kg/m^3) and λ_p is thermal conductivity of product (W/m°C).

2.5. Initial and boundary conditions

Using the initial and boundary conditions for heat and mass transfer, the governing equations (1) and (2) are solved for products subjected to convective drying with hot air [19], [40], [26].

- Initial conditions

$$t=0\begin{cases}X_p(x,y,t)=X_p(x,y,0)=X_{p0}\\T_p(x,y,t)=T_p(x,y,0)=T_{p0}\end{cases}$$

- Boundary conditions (BC)

On the surface: ($j=N_y$)

$$\lambda_p\left.\frac{\partial T_p}{\partial y}\right|_{y=0}=h\left(T_a-T_p\right)+h_m\left(X_p-X_a\right)*L_v \tag{3}$$

$$D_{eff}\left.\frac{\partial X_p}{\partial y}\right|_{y=0}=h_m\left(X_p-X_a\right) \tag{4}$$

At the leading edge $(i=1)$

$$\lambda_p\left.\frac{\partial T_p}{\partial x}\right|_{x=0}=h\left(T_a-T_p\right)+h_m\left(X_p-X_a\right)*L_v \tag{5}$$

$$D_{eff}\left.\frac{\partial X_p}{\partial x}\right|_{x=0}=h_m\left(X_p-X_a\right) \tag{6}$$

At the trailing edge $(i=N_y)$

$$\lambda_p\left.\frac{\partial T_p}{\partial x}\right|_{x=L}=h\left(T_a-T_p\right)+h_m\left(X_p-X_a\right)*L_v \tag{7}$$

$$D_{eff}\left.\frac{\partial X_p}{\partial x}\right|_{x=L}=h_m\left(X_p-X_a\right) \tag{8}$$

In the median plane $(j=1)$

$$-\lambda_p\left(\frac{\partial T_p}{\partial x}+\frac{\partial T_p}{\partial y}\right)=0 \tag{9}$$

$$-D_{eff}\left(\frac{\partial X_p}{\partial x}+\frac{\partial X_p}{\partial y}\right)=0 \tag{10}$$

Where

$$L_v=4.1868*\left(597-0.56*T_p\right)\ (11);\ X_a=\rho_a C_{va} \tag{12}$$

$$C_{va}=2.1667*10^{-3}*\frac{Hr}{100}*\frac{P_{vs}(T_a)}{T_a} \tag{13}$$

$$\text{With } P_{vs}=Exp\left(\frac{5.8*10^3}{T_a}+1.391-4.864*10^{-2}T_a+4.176*10^{-5}T_a^{\,2}-1.445*10^{-8}T_a^{\,2}+6.545*\ln\left(T_a\right)\right) \tag{14}$$

Where C_{va} is mass fraction of water vapor in air; Hr is relative humidity (%); h is convective heat transfer coefficient ($W/m^2°C$); h_m is Convective mass transfer coefficient (m/s); L_v is latent heat of vaporization (kJ/kg) ; P_{vs} is saturation vapor pressure (bar); T_a is temperature of air (°C); X_a is moisture content of air (kg/m^3) and ρ_a is density of air (kg/m^3).

From the dry-base moisture content (X_p), the moisture ratio (MR) and drying rate (V_s) are calculated from the following correlations [41], [42].

$$MR=\frac{X_p}{X_{p0}} \tag{15}$$

$$V_s = \frac{dX_p}{dt} = \frac{X_{pt} - X_{pt+dt}}{dt} \quad (16)$$

The heat transfer coefficient (h) and mass transfer coefficient (hm) in the above equations can be determined from the average Nusselt and Sherwood numbers for laminar or turbulent flow over flat plates as follows [43].

- Laminar flow

$$Nu = \frac{h*L}{\lambda_a} = 0.664\,\mathrm{Re}^{0.5}\,\mathrm{Pr}^{0.33} \quad (17)$$

$$Sh = \frac{h_m*L}{D_a} = 0.664\,\mathrm{Re}^{0.5}\,Sc^{0.33} \quad (18)$$

- Turbulent flow

$$Nu = \frac{h*L}{\lambda_a} = 0.0592\,\mathrm{Re}^{0.5}\,\mathrm{Pr}^{0.33} \quad (19)$$

$$Sh = \frac{h_m*L}{D_a} = 0.0592\,\mathrm{Re}^{0.8}\,Sc^{0.33} \quad (20)$$

Where D_a is diffusion coefficient of water vapor (m^2/s); L is product length (m); Re is Reynolds number; Sc is Schmidt number; Sh is Sherwood number, Nu is Nusselt numbers and λ_a is thermal conductivity of air (W/m°C).
Papaya, characterized by its associated thermophysical parameters, is used as a product for the simulation of the mathematical model. The following table lists the simulation parameters used:

Table 1: Simulation Parameters

Parameters	Symbols	Units	Values
Air temperature	T_a	°C	40 - 50 - 60
Airflow velocity	V_a	m/s	0.2-1-2
Relative humidity of the air	Hr	%	50
Initial moisture content of the papaya	X_{p0}	%	82.64
Initial product temperature	T_{p0}	°C	25

The thermo-physical properties of air and product are essential parameters when modeling the drying process. The thermo-physical properties of air used in this work were those proposed by Mabrouk [44]. The thermo-physical properties of papaya slices proposed by Fouakeu-nanfack et al. [16] for mass diffusivity coefficient and by Lemus-Mondaca et al. [45] for thermal diffusivity coefficient parameters are given by the following equations:

- Effective diffusivity coefficient

$$D_{eff}(T_a)\big|_{40^\circ C-60^\circ C} = 8.1717*10^{-8}*Exp\left(-\frac{16.2622}{8.314(T_a+273.15)}\right) \quad (21)$$

- Density

$$\rho_p(T_a)\big|_{10^\circ C-90^\circ C} = 1.03*10^3 - 7.9*10^{-3}T_a - 3.69*10^{-3}T_a^2 \quad (22)$$

- Specific heat

$$C_{pp}(T_a)\big|_{10^\circ C-90^\circ C} = 3.93*10^3 + 8.66*10^{-2}T_a + 4.53*10^{-3}T_a^2 \quad (23)$$

- Thermal conductivity

$$\lambda_p(T_a)\big|_{10^\circ C-90^\circ C} = 5.52*10^{-1} + 1.73*10^{-3}T_a - 6.48*10^{-6}T_a^2 \quad (24)$$

2.6. Validation of the model

To validate the theoretical results obtained in this work, they were compared with the experimental results presented by Lemus-Mondaca et al. [45]. The thermo-physical parameters of the model used are given by Lemus-Mondaca et al. [45]. The simulation conditions are identical to the experimental conditions of convective drying for papaya. The validation of the results is done by calculating the average relative error between experimental and theoretical values from the following relation [38]:

$$E(\%) = \sum_{i=1}^{n} \frac{\left|Y_{\exp} - Y_{sim}\right|}{Y_{\exp}} \frac{100}{n} \quad (25)$$

Où Y_{exp} is the experimental data; Y_{sim} is simulated data and n is number of observations.
The heat and moisture transfer equations given in (1) and (2) under the corresponding initial and boundary conditions were discretized using the implicit finite-difference method. These were coupled and solved simultaneously using MATLAB 2014 software.

3. Results and discussion

3.1. Validation of the model

The following figure 2 shows the evolution of the simulated and experimental moisture ratio of papaya. It is observed that there is a very good adequacy between the theoretical and experimental results. The result shows a mean relative error of 2.92% for the product's moisture ratio. The model is validated when the average relative error is generally lower or equal to 3%. With the value presented in this study being clearly in this range, we can in view of this result, conclude that the transfer model used allows for more accurate results.

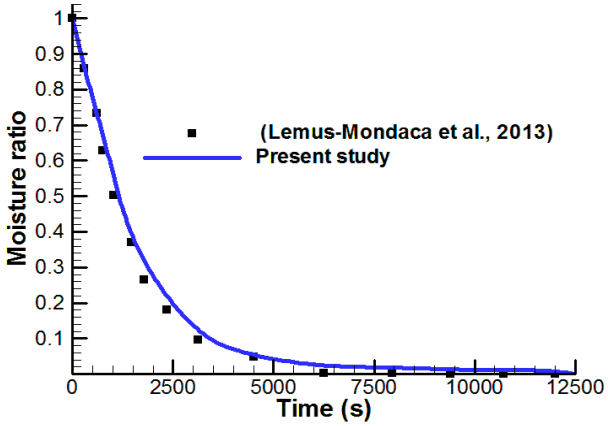


Fig. 2: Comparison of the Moisture Ratio of the Present Study Simulated with the Experimental Results of [16] (Ta = 60°C, Va = 1.5 M/S, E =10 Mm Et L = 30 Mm, Hr = 57%)

3.2. Influence of the drying air temperature

Figure 3 shows the profile of the moisture ratio of the product as a function of time under the influence of the drying air temperature. The figure shows that the moisture ratio is highest at the start of drying and decreases with time at different drying air temperatures. The figure shows that the three curves for moisture ratio merge during the first 12 minutes of drying, indicating the product's heat-up phase. The figure also shows that after 8 hours of drying, the moisture ratio is 0.181, 0.122 and 0.098 for temperatures of 40°C, 50°C and 60 °C, respectively. This result shows that the moisture content decreases by 48.686% and 24.161% for passages from 40°C to 50°C and from 50°C to 60°C, respectively. This rate of decrease for the 50°C to 60°C passage indicates low water evaporation power compared to that for the 40°C to 50°C passage. This low water evaporation power is justified by the closeness of the moisture ratio curves at 50°C and 60°C, showing that the drying air temperature is close to the critical drying temperature of the product. This result is similar to that obtained by Ambarita and Nasution [20] and Matuam et al. [26] when modeling convective drying of mango.

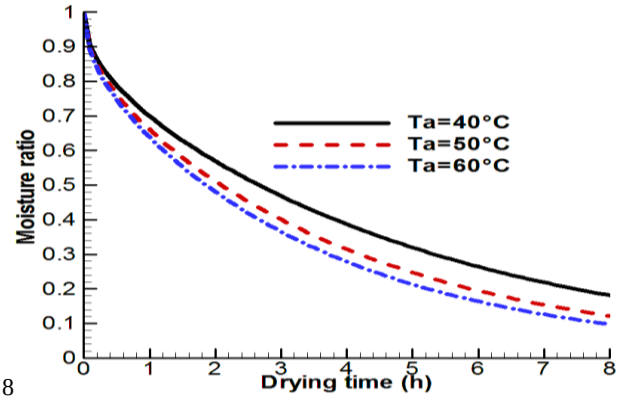


Fig. 3: Profile of the Moisture Ratio of the Product as A Function of Time (V_a =1m/S, E = 0.006m, Hr = 50%).

Figure 4 shows the product temperature profile as a function of time under the influence of the drying air temperature. The figure shows that the product temperature is low at the start of drying and rises as a function of time for different drying air temperatures. This result shows that the product temperature rises exponentially from its initial value of 25°C to 36.614°C, 48.686°C and 58.995°C, tending towards 40°C, 50°C and 60 °C, respectively. This behavior is strongly influenced by product density. A similar result was observed in the work of Villa-Corrales et al. [34] and Erko et al. [19] who respectively modeled mango and potato during convective drying.

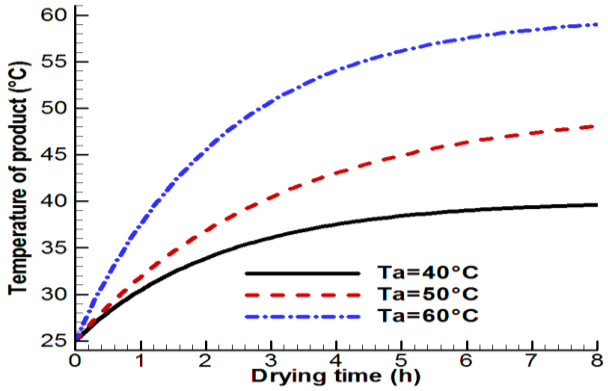


Fig. 4: Profile of Product Temperature as A Function of Time (Va =1m/S, E = 0.006m, Hr = 50%).

Figure 5 shows the profile of drying rate as a function of time under the influence of drying air temperature. The figure shows a sharp decrease in drying rate as a function of time for the different drying air temperatures. Drying rate reaches its maximum at 0.0075 kg/kg $_{db.min}$, 0.0062 kg/kg $_{db.min}$ and 0.0054 kg/kg $_{db.min}$ for drying temperatures of 40°C, 50°C and 60°C, respectively. It can be seen from this figure that after 3 hours and 40 minutes of drying, the quantity of water to be evaporated at 40°C is higher than at 50°C and 60°C. But this tendency is reversed after 3 hours and 40 minutes of drying. This behavior may be due to the phenomenon of crusting or the unavailability of water in the product, which is in agreement with the work of Pandith [46] and Fouakeu-nanfack et al. [39] when characterizing convective drying of papaya.

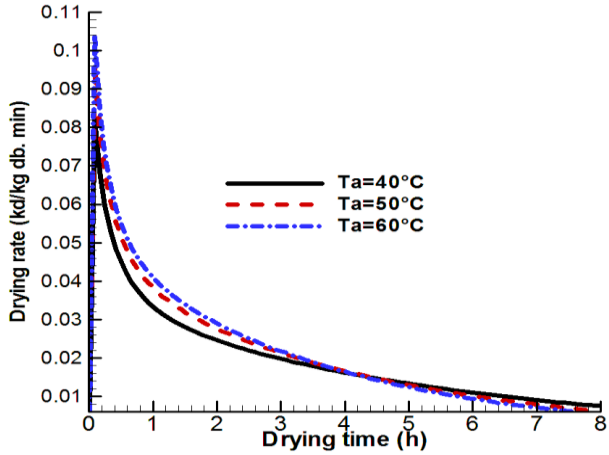


Fig. 5: Profile of Drying Rate as A Function of Time (Va =1m/S, E = 0.006m, Hr = 50%).

3.3. Influence of drying airflow velocity

Figure 6 shows the profile of moisture ratio as a function of time under the influence of drying airflow velocity. This graph shows that, for the various drying airflow velocities, the moisture ratio decreases as a function of time with extremely small variations, resulting in a confusion of curves. This finding demonstrates that airflow velocity during papaya drying is not particularly important because internal resistance to moisture transfer is thought to be the main factor. This result conforms with the modeling of agricultural products under convective drying done by Tavakolopour [47].

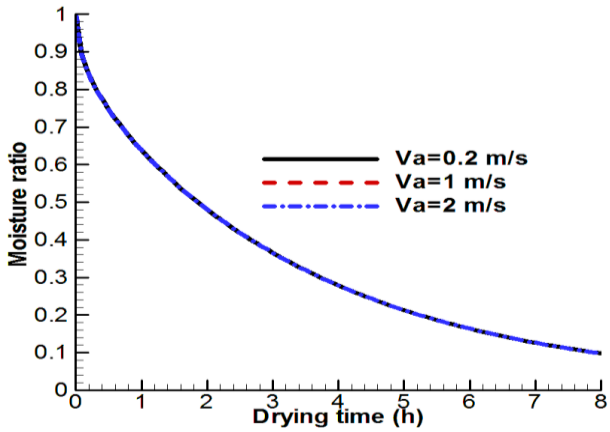


Fig. 6: Profile of Moisture Ratio as A Function of Time (T_a= 60°C, E = 0.006m, Hr = 50%).

3.4. Influence of product thickness

Figure 7 shows the profile of moisture ratio as a function of time under the influence of product thickness. The figure shows that the moisture ratio is highest at the start of drying and decreases as a function of time for different product thicknesses. The figure shows that after 8 hours of drying, the moisture ratio is 0.016, 0.098 and 0.242 for thicknesses of 4 mm, 6 mm and 8 mm, respectively. It was also found that before thermal equilibrium of the product, the moisture ratio decreased by 2.17% with an increase of 2 mm in product thickness. This result can be explained by the fact that the path of water diffusion from the interior to the surface of the product is longer. It is therefore verified that the reduction in product thickness promotes faster drying of agri-food products, which is in conformity with the work of Villa-Corrales et al. [34] where the moisture ratio decreased by 4.5% with the increase of one millimeter in product thickness during mango drying.

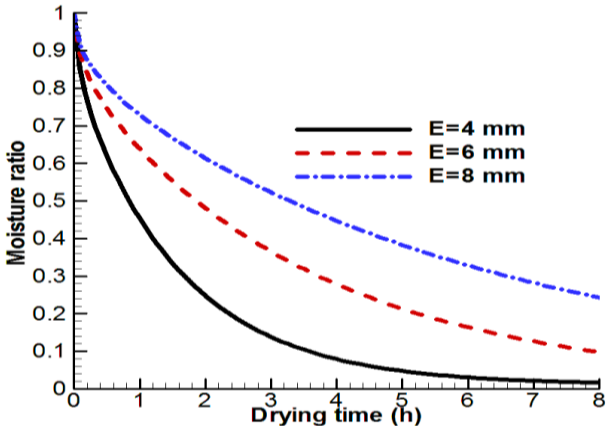


Fig. 7: Profile of Moisture Ratio as A Function of Time (T_a = 60°C, V_a = 1m/S, Hr = 50%).

Figure 8 shows the product temperature profile as a function of time under the influence of product thickness. It can be seen from this figure that the product temperature is minimal at the start of drying and increases as a function of time for the different product thicknesses. This result shows that the product temperature rises exponentially from its initial value of 25°C to reach 59.219°C, 57.237°C and 54.744°C for thicknesses of 4 mm, 6 mm and 8 mm, respectively. It is justified that the thickness of the product is a parameter that significantly influences the drying of food products since the path of water diffusivity depends on it.

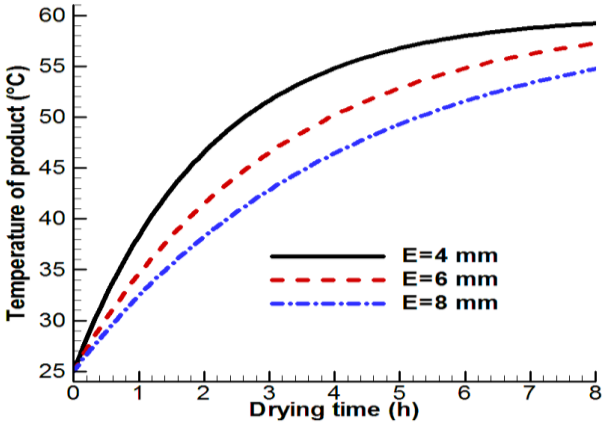


Fig. 8: Profile of Product Temperature as A Function of Time (T_a = 60°C, V_a = 1m/S, Hr = 50%).

Figure 9 shows the profile of drying rate as a function of time under the influence of product thickness. The figure shows a rapid decrease in drying rate as a function of time for different product thicknesses. The drying rate reaches its maximum at 0.00079 kg/kg $_{db.min}$, 0.0054 kg/kg $_{db.min}$ and 0.0081 kg/kg $_{db.min}$ for product thicknesses of 4 mm, 6 mm and 8 mm, respectively. The figure shows that after 2 hours and 25 minutes of drying, the quantity of water to be evaporated for the 4 mm curve is higher than for the 6 mm and 8 mm curves. This tendency reverses between 2 hours and 25 minutes, and 4 hours and 30 minutes, showing that the quantity of water to evaporate becomes more important for the 6 mm curve. After 4 hours and 30 minutes of drying, another tendency is observed, showing that the quantity of water to be evaporated becomes more important for the 8 mm curve.

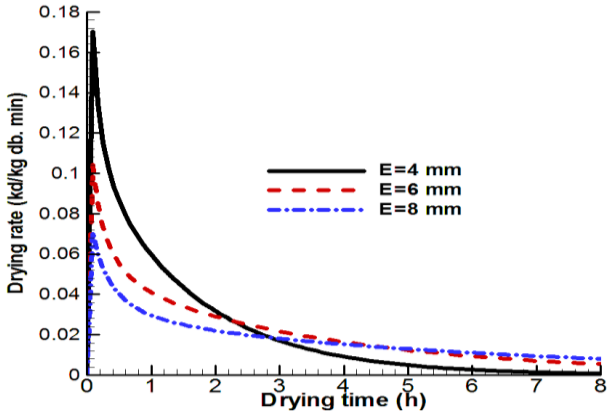


Fig. 9: Profile of Drying Rate as A Function of Time (T_a = 60°C, V_a = 1m/S, Hr = 50%).

3.5. Moisture content distribution profiles in the product

Figure 10 shows the distribution of moisture content in the product as a function of both space and drying time. After 8 hours of drying, this graph shows the evolution of the product's moisture content from the surface to the center. As drying time increases, it can be seen that moisture content gradients from the product's surface to its center decrease, although the moisture content close to the product's center drops gradually [21]. Similar results were found in the work of Ngouem et al. [39], who described cocoa shrinkage in order to include it in transfer models.

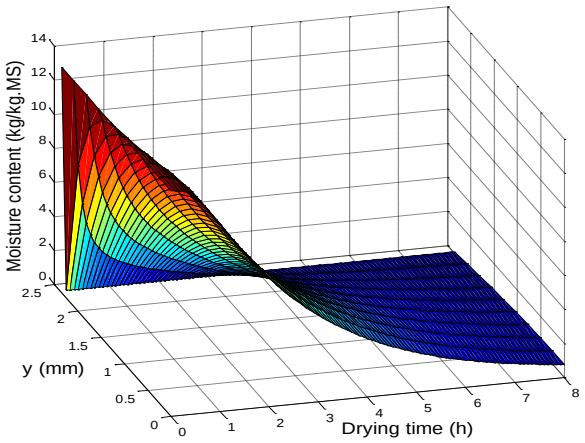


Fig. 10: 3D Profile of Distribution of Moisture Content (T_a = 60°C, V_a = 1.76m/S, E = 0.005m, Hr = 35%).

Figure 11 shows the temperature distribution of the product as a function of both space and drying time. It is observed that the product temperature rises from its initial value and tends towards the drying air temperature as a function of time. However, It can be seen from this figure that the temperature gradient from the surface to the center of the product can be considered insignificant, and it can be assumed that the product is heated isothermally [21]. This behavior is due to the low specific heat of papaya. A similar result was observed in the work of Ngouem et al. [39], who characterized the shrinkage of cocoa with the aim of taking it into account in transfer models.

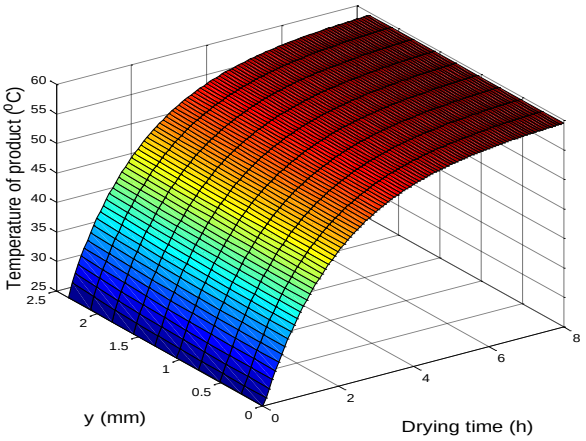


Fig. 11: 3D Profile of Distribution of Product Temperature (Ta = 60°C, Va = 1.76m/S, E = 0.005m, Hr = 35%).

3.6. Comparison of results

The following figure12 shows the comparison of numerical and experimental simulation results of moisture ratio and product temperature as a function of time. Looking at the curves in this figure, we observe that the calculated moisture ratio is higher than the measured

temperature. We find that for the moisture ratio, the mean relative errors are 5.21% and 3.89% for the model without and with boundary conditions set at the leading and trailing edges, respectively. Similarly, results showed that for product temperature, mean relative errors were 4.35% and 3.61% for the model without and with boundary conditions set at the leading and trailing edges, respectively. Comparison of predicted models with experimental data satisfactorily demonstrates that incorporating leading-edge and trailing-edge boundary conditions into a transfer model provides a better prediction of drying kinetics than the model without leading-edge and trailing-edge boundary conditions. Average relative errors of over 3% can be explained by the fact that the global transfer coefficients used in these models do not reflect the actual behavior of transfers during drying, hence the need to take into account the parietal boundary layer in transfer models.

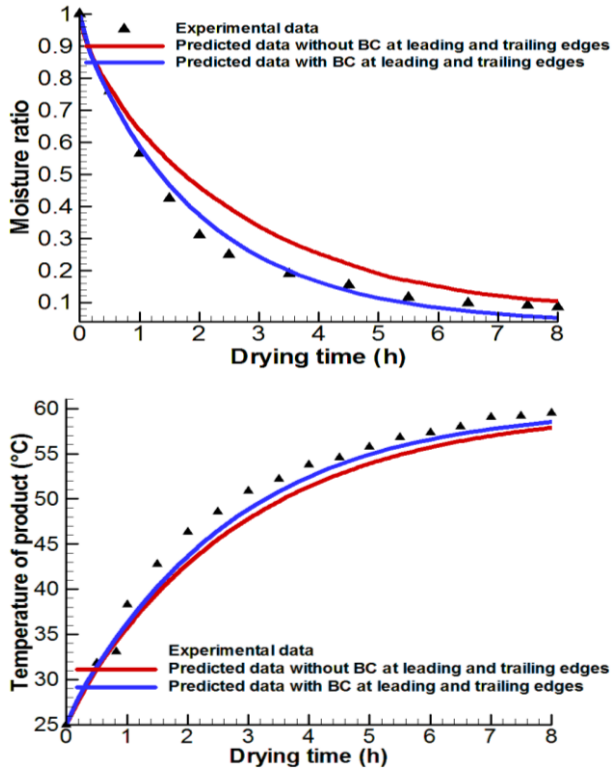


Fig. 12: Numerical and Experimental Simulation of Moisture Ratio and Temperature of Product (T_a = 60°C, V_a = 1.76m/S, E = 0.005m, Hr = 35%).

4. Conclusions

The drying of papaya in a parallel airflow was simulated in the current work to predict convective heat and mass transfer. The purpose of this work was to improve the prediction of papaya drying kinetics by considering the boundary conditions at the leading and trailing edges in the coupled and simultaneous resolution of the heat and mass transfer equations. These papaya slices were cut into slices and set on a support that was 30 cm long and 5 mm thick. The implicit finite-difference method was used to discretize the Luikov equations for this transfer model, and they were then simultaneously solved in Matlab 2014. Simulations of papaya drying were carried out under the influence of drying air temperature, airflow velocity and product thickness. The predicted data from this model were compared to the experimental data. The predicted data from this model were compared to the experimental data. The results showed that for the moisture ratio, the mean relative errors were 5.21% and 3.89% for the model without and with boundary conditions set at the leading and trailing edges, respectively. Similarly, the results showed that for product temperature, the mean relative errors were 4.35% and 3.61% for the model without and with boundary conditions set at the leading and trailing edges, respectively. Comparison of the predicted models with the experimental data satisfactorily demonstrated that incorporating the leading and trailing edge boundary conditions in a transfer model enabled better prediction of drying kinetics than the model without the leading and trailing edge boundary conditions. Average relative errors of over 3% can be explained by the fact that the global transfer coefficients used in these models do not reflect the actual behavior of transfers during drying, hence the need to take into account the parietal boundary layer in transfer models.

Acknowledgements

The authors would like to thank the Doctoral Training Unit – Applied Physics and Engineering of the National School of Agro-Industrial Sciences (ENSAI) of the University of Ngaoundere for having provided us with the experimental device that allowed us to carry out the tests.

References

[1] F. Akter, R. Muhury, A. Sultana, et U. K. Deb, « A Comprehensive Review of Mathematical Modeling for Drying Processes of Fruits and Vegetables », International Journal of Food Science, vol. 2022, p. 1-10, 2022, https://doi.org/10.1155/2022/6195257.

[2] A. M. Castro, E. Y. Mayorga, et F. L. Moreno, « Mathematical modelling of convective drying of fruits: A review », Journal of Food Engineering, vol. 223, p. 152-167, 2018, https://doi.org/10.1016/j.jfoodeng.2017.12.012.

[3] O. Prakash et A. Kumar, Solar Drying Technology: Concept, Design, Testing, Modeling, Economics, and Environment. Springer, 2017. https://doi.org/10.1007/978-981-10-3833-4.

[4] A. O. Omolola, A. I. Jideani, et P. F. Kapila, « Quality properties of fruits as affected by drying operation », Critical reviews in food science and nutrition, vol. 57, no 1, p. 95-108, 2017, https://doi.org/10.1080/10408398.2013.859563.

[5] D. A. Tzempelikos, D. Mitrakos, A. P. Vouros, A. V. Bardakas, A. E. Filios, et D. P. Margaris, « Numerical modeling of heat and mass transfer during convective drying of cylindrical quince slices », Journal of Food Engineering, vol. 156, p. 10-21, 2015, https://doi.org/10.1016/j.jfoodeng.2015.01.017.

[6] N. G. A. Fouakeu, F. A. Tetang, M. Edoun, A. Kuitche, et B. Zeghmati, « A contribution to a numerical characterization of the thermal transfers in a saw tooth solar collector », International Journal of Thermal Technologies, vol. 9, no 3, p. 200-206, 2019.

[7] A. M. Castro, L. E. Díaz, M. X. Quintanilla-Carvajal, E. Y. Mayorga, et F. L. Moreno, « Convective drying of feijoa (Acca sel-lowiana Berg): A study on bioactivity, quality, and drying parameters », LWT, vol. 186, p. 115209, 2023, https://doi.org/10.1016/j.lwt.2023.115209.

[8] A. Stegou-Sagia et D. Fragkou, « Influence of drying conditions and mathematical models on the drying curves and the moisture diffusivity of mushrooms », Journal of Thermal Engineering, vol. 1, no 4, p. 235-244, 2015, https://doi.org/10.18186/jte.65158.

[9] J. A. K. M. Fernando et A. D. U. S. Amarasinghe, « Drying kinetics and mathematical modeling of hot air drying of coconut coir pith », SpringerPlus, vol. 5, no 1, p. 807, juin 2016, https://doi.org/10.1186/s40064-016-2387-y.

[10] A. S.-S. Stegou–Sagia et A. Fragkou, « Thin layer drying modeling of apples and apricots in a solar-assisted drying system », Journal of Thermal Engineering, vol. 4, no 1, p. 1680-1691, 2018, https://doi.org/10.18186/journal-of-thermal-engineering.364909.

[11] O. Badaoui, S. Hanini, A. Djebli, B. Haddad, et A. Benhamou, « Experimental and modelling study of tomato pomace waste drying in a new solar greenhouse: Evaluation of new drying models », Renewable energy, vol. 133, p. 144-155, 2019, https://doi.org/10.1016/j.renene.2018.10.020.

[12] F. A. Tetang, E. Marcel, et K. Alexis, « Intermittent Drying of Mango Slices (Mangifera indica L.)" Amelie": A New Model », American Journal of Food Science and Technology, vol. 8, no 3, p. 81-86, 2020.

[13] A. Tom, D. Bruneau, et N. Djongyang, « Drying kinetics of beef meat: Modeling by the isenthalpe mass flux method », J Food Process Eng, vol. 44, no 4, avr. 2021, https://doi.org/10.1111/jfpe.13647.

[14] S. Keskes, S. Hanini, M. Hentabli, et M. Laidi, « Artificial Intelligence and Mathematical Modelling of the Drying Kinetics of Pharmaceutical Powders. », Kemija u Industriji, vol. 69, 2020, https://doi.org/10.15255/KUI.2019.038.

[15] A. Kushwah, G. Mk, A. Kumar, et P. Singh, « Application of ANN and prediction of drying behavior of mushroom drying in side hybrid greenhouse solar dryer: An experimental validation », Journal of Thermal Engineering, vol. 8, no 2, p. 221-234, 2021, https://doi.org/10.18186/thermal.1086189.

[16] G. A. Fouakeu-nanfack, G. T. N. Wilfred, M. Balbine, E. Marcel, et Z. Belkacem, « Experimental characterization of convective drying of papaya (Carica papaya L.) to licking airflow », International Journal of Current Engineering and Technology, 2023.

[17] J. Wang et al., « Study on Cut Tobacco Drying Process Based on HS-GC/MS: Principal Component Analysis, Similarity Analy-sis, Drying Conditions, and Drying Mechanism », Journal of Chemistry, vol. 2023, p. 1-7, 2023, https://doi.org/10.1155/2023/5772916.

[18] A. O. Oladejo et al., « Influence of ultrasound-pretreated convective drying of Roselle (Hibiscus sabdariffa L) leaves on its dry-ing kinetics and nutritional quality », Scientific African, vol. 20, p. e01704, juill. 2023, https://doi.org/10.1016/j.sciaf.2023.e01704.

[19] K. G. Erko, A. H. Taye, et W. C. Hofacker, « Numerical Modeling of Coupled Heat and Mass Transfer with Moving Boundary during Convective Drying Of Potato Slices », International Journal of Scientific & Engineering Research, vol. 8, no 11, p. 71-78, 2017.

[20] H. Ambarita et A. H. Nasution, « A numerical solution to simultaneous heat and mass transfer of convective drying of food », J. Phys.: Conf. Ser., vol. 1116, no 3, p. 032002, déc. 2018, https://doi.org/10.1088/1742-6596/1116/3/032002.

[21] V. Chasiotis, D. Tzempelikos, D. Mitrakos, et A. Filios, « Numerical and experimental analysis of heat and moisture transfer of Lavandula x allardii leaves during non-isothermal convective drying », Journal of Food Engineering, vol. 311, p. 110708, 2021, https://doi.org/10.1016/j.jfoodeng.2021.110708.

[22] M. Y. Nasri et A. Belhamri, « A Semi-Empirical Approach for Predicting the Effects of Shrinkage on the Convective Mass Transfer Evolution During the Solar Drying of Foodstuffs. », International Journal of Heat & Technology, vol. 41, no 2, p. 439-446, 2023, https://doi.org/10.18280/ijht.410219.

[23] W. P. Da-Silva, C. M. e Silva, et J. P. Gomes, « Drying description of cylindrical pieces of bananas in different temperatures using diffusion models », Journal of Food Engineering, vol. 117, no 3, p. 417-424, 2013, https://doi.org/10.1016/j.jfoodeng.2013.03.030.

[24] J. A. Esfahani, H. Majdi, et E. Barati, « Analytical two-dimensional analysis of the transport phenomena occurring during con-vective drying: apple slices », Journal of Food Engineering, vol. 123, p. 87-93, 2014, https://doi.org/10.1016/j.jfoodeng.2013.09.019.

[25] N. Shahari, H. A. Hasnan, A. Y. Hanan, et N. N. Ishak, « Analysis of two-dimensional (2d) fruit drying process through heat and mass transfer model », in IOP Conference Series: Materials Science and Engineering, IOP Publishing, 2019, p. 012024. https://doi.org/10.1088/1757-899X/477/1/012024.

[26] B. Matuam, N. Gnepie, J. Fotsa, A. Tetang, M. Edoun, et E. Alexis Kuitche, « Numerical Simulation of Heat and Moisture Transfer in Corrugated Walls Dryer », AE, vol. 7, no 1, p. 1-10, 2023, https://doi.org/10.11648/j.ae.20230701.11.

[27] L. Lagunez-Rivera, I. I. Ruiz-López, M. A. García-Alvarado, et M. A. Salgado-Cervantes, « Mathematical simulation of the ef-fective diffusivity of water during drying of papaya », Drying Technology, vol. 25, no 10, p. 1633-1638, 2007, https://doi.org/10.1080/07373930701590772.

[28] B. Mocelin et al., « Mathematical modeling of thin layer drying of papaya seeds in a tunnel dryer using particle swarm optimiza-tion method », Particulate Science and Technology, vol. 32, no 2, p. 123-130, 2014, https://doi.org/10.1080/02726351.2013.839015.

[29] M. Torki-Harchegani, D. Ghanbarian, et M. Sadeghi, « Estimation of whole lemon mass transfer parameters during hot air drying using different modelling methods », Heat and mass transfer, vol. 51, no 8, p. 1121-1129, 2015, https://doi.org/10.1007/s00231-014-1483-1.

[30] G. L. Dotto, L. Meili, E. H. Tanabe, D. P. Chielle, et M. F. P. Moreira, « Evaluation of the mass transfer process on thin layer drying of papaya seeds from the perspective of diffusive models », Heat and Mass Transfer, vol. 54, no 2, p. 463-471, 2018, https://doi.org/10.1007/s00231-017-2128-y.

[31] R. Muhury, F. Akter, et U. K. Deb, « Simulation of the Heat and Mass Transfer Occurring During Convective Drying of Mango Slices », in Intelligent Computing & Optimization: Proceedings of the 4th International Conference on Intelligent Computing and Optimi-zation 2021 (ICO2021) 3, Springer, 2022, p. 751-761. https://doi.org/10.1007/978-3-030-93247-3_72.

[32] P. Chen et al., « A Heat and Mass Transfer Model of Peanut Convective Drying Based on a Two-Component Structure », Foods, vol. 12, no 9, Art. no 9, janv. 2023, https://doi.org/10.3390/foods12091823.

[33] A. S. Souza, T. C. Souza Pinto, A. M. Sarkis, T. F. D. Pádua, et R. Béttega, « Convective drying of iron ore fines: A CFD model validated for different air temperatures and air velocities », Drying Technology, p. 1-16, août 2023, https://doi.org/10.1080/07373937.2023.2252050.

[34] L. Villa-Corrales, J. J. Flores-Prieto, J. P. Xamán-Villaseñor, et E. García-Hernández, « Numerical and experimental analysis of heat and moisture transfer during drying of Ataulfo mango », Journal of food engineering, vol. 98, no 2, p. 198-206, 2010, https://doi.org/10.1016/j.jfoodeng.2009.12.026.

[35] G. Takamte, M. Edoun, L. Monkam, A. Kuitche, et R. Kamga, « Numerical Simulation of Convective Drying of Mangoes (man-gifera Indica L.) Under Variable Thermal Conditions », International Journal of Thermal Technologies, vol. 3, no 2, p. 48-52, 2013.

[36] T. J. Afolabi et S. E. Agarry, « Mathematical modeling and simulation of the mass and heat transfer of batch convective air drying of tropical fruits », Chem. Process Eng. Res, vol. 23, no 1, 2014.

[37] X.-L. Yu et al., « Multistage relative humidity control strategy enhances energy and exergy efficiency of convective drying of carrot cubes », International Journal of Heat and Mass Transfer, vol. 149, p. 119231, mars 2020, https://doi.org/10.1016/j.ijheatmasstransfer.2019.119231.

[38] G. A. Fouakeu-nanfack, S. Kewou, F. J. Ngouem, A. T. Fokone, M. Edoun, et B. Zeghmati, « Numerical and experimental char-acterization of internal heat and mass transfer during convective drying of papaya (Carica papaya L.) in a drying air stream », International Journal of Energetica, vol. 8, no 2, p. 1-10, déc. 2023, Consulté le: 9 janvier 2024. [En ligne]. Disponible sur: https://www.ijeca.info/index.php/IJECA/article/view/221.

[39] M. K. Kosheleva, S. P. Rudobashta, O. R. Dornyak, et V. M. Dmitriev, « Convective Drying of Flat Fibrous Materials », J Eng Phys Thermophy, vol. 96, no 4, p. 988-993, juill. 2023, https://doi.org/10.1007/s10891-023-02761-6.

[40] F. J. Ngouem, M. Edoun, L. Monkam, et A. Tetang, « Simulation of Convective Drying with Shrinkage using the Finite Window Method: Application and Validation », American Scientific Research Journal for Engineering, Technology, and Sciences (ASRJETS), vol. 78, no 1, p. 39-49, 2021.

[41] I. Doymaz et A. S. Kipcak, « Effect of pre-treatment and air temperature on drying time of cherry tomato », Journal of Thermal Engineering, vol. 4, no 1, p. 1648-1655, 2018. https://doi.org/10.18186/journal-of-thermal-engineering.364489.
[42] S. Nansereko, J. Muyonga, et Y. B. Byaruhanga, « Influence of Drying Methods on Jackfruit Drying Behavior and Dried Prod-ucts Physical Char-acteristics », International Journal of Food Science, vol. 2022, p. e8432478, sept. 2022, https://doi.org/10.1155/2022/8432478.
[43] R. Golestani, A. Raisi, et A. Aroujalian, « Mathematical modeling on air drying of apples considering shrinkage and variable diffusion coefficient », Drying Technology, vol. 31, no 1, p. 40-51, 2013, https://doi.org/10.1080/07373937.2012.714826.
[44] S. B. Mabrouk, B. Khiari, et M. Sassi, « Modelling of heat and mass transfer in a tunnel dryer », Applied thermal engineering, vol. 26, no 17-18, p. 2110-2118, 2006, https://doi.org/10.1016/j.applthermaleng.2006.04.007.
[45] R. A. Lemus-Mondaca, C. E. Zambra, A. Vega-Gálvez, et N. O. Moraga, « Coupled 3D heat and mass transfer model for numer-ical analysis of drying process in papaya slices », Journal of Food Engineering, vol. 116, no 1, p. 109-117, mai 2013, https://doi.org/10.1016/j.jfoodeng.2012.10.050.
[46] J. A. Pandith, « Induction heating assisted foam mat drying of papaya pulp: drying kinetics, drying modeling, and effects on qual-ity attributes », Agricultural Engineering International: CIGR Journal, vol. 20, no 2, p. 206-215, 2018.
[47] H. Tavakolipour, « Drying kinetics of pistachio nuts (Pistacia vera L.) », World Applied Sciences Journal, vol. 12, no 9, p. 1639-1646, 2011.